DRYING AND DRYERS

Anthony J. Hlinak
Bradley A. Clark
Pharmacia, Skokie, Illinois, U.S.A.

INTRODUCTION

Many pharmaceutical operations, including those used to produce active pharmaceutical ingredients and excipients, use water or organic solvents as essential processing aids. However, the continued presence of these processing aids may hamper downstream manufacturing operations or compromise the safety and stability of the final pharmaceutical product. Drying is a common unit operation used to reduce the levels of water or organic solvent in pharmaceutical materials to acceptable levels. Drying requires the use of a manufacturing firm'–s scarce resources: facilities, equipment, utilities, human labor, and time. Thus, there is often economic pressure to select aggressive drying conditions in an effort to minimize cycle times and increase throughput. However, the drying rate can impact the properties, functionality, and quality of the material being dried. Thus, the practitioner must balance the economic pressure with the quality and performance needs of the product.

In general terms, drying can be described by three processes operating simultaneously. The first process is energy transfer from an external source to the water or organic solvent in the material. The second process is the phase transformation of the water or organic solvent from a liquid or liquid-like state to a vapor state. The third process is the transfer of the vapor generated away from the pharmaceutical material and out of the drying equipment. Analysis of the drying process is complicated by the fact these three processes are coupled to each other, and all three need to be considered simultaneously.

THEORY

Heat Transfer

For most equipment designs, the energy transferred is in the form of heat. Heat flows naturally in the direction of decreasing temperature and is known to transfer by three distinct mechanisms. The first, conduction, involves purely molecular scale transfers of kinetic energy and can be modeled in one dimension in the steady state using Fourier'–s equation of heat conduction (1):

$$q_k = -kA\frac{dT}{dx} \tag{1}$$

where q_k is the rate of energy transferred by the conductive mechanism (calories/s), k the thermal conductivity of the transferring medium (calories/s/cm/°C), A the transfer area (cm^2), and

$$\frac{dT}{dx}$$

is the temperature gradient in the direction of transfer (°C/cm).

For the simple case of steady one-dimensional heat flow through a homogeneous medium with parallel, planer boundaries held at fixed temperatures, Eq. 1 can be integrated to yield

$$q_k = kA\frac{(T_s - T_i)}{\ell} \tag{2}$$

where T_s,T_i are the exposed surface and interface temperatures, respectively (°C) and ℓ is the thickness of the material layer (cm).

Although derived assuming the simplest of conditions, Eq. 2 can be used to analyze a variety of drying situations as illustrated in Fig. 1, including cases involving modest curvature, as a reasonable approximation. Solutions for more complex cases, including nonplaner geometries, nonsteady state, and complex boundary conditions can be found in classic texts on the subject (2).

A useful concept, known as thermal resistance, can be derived from Eq. 2 by a simple redefinition of terms:

$$q_k = \frac{(T_s - T_i)}{R_k} \tag{3}$$

Here

$$R_k = \frac{\ell}{kA}$$

is the thermal resistance. Eq. 3 takes the functional form of Ohm'–s law in electrical circuit theory, with

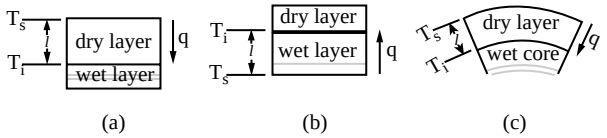

Fig. 1 Application of Eq. 2 to (a) direct heating of a static solids bed, (b) indirect heating of a static solids bed, and (c) fluid bed-drying of a spherical particle.

the temperature difference playing the role of voltage difference, energy flow in the role of current flow, and thermal resistance in the role of electrical resistance. This form emphasizes the importance of the temperature difference as the driving force behind thermal transport and permits the physical factors that make up the thermal resistance to be broken down in detail. Because of this analogy with Ohm'–s law, thermal "circuits" can be constructed to handle complex cases involving simultaneous transfer with multiple heat transfer mechanisms or sources and the techniques developed for electrical circuits can be used to simplify the analysis.

In the second heat transfer mechanism, convection, molecular scale transfers of kinetic energy are augmented by the macroscopic movement of a fluid transfer medium. Convection is most important as the mechanism of transfer between the solid surface of a static bed or an individual suspended particle and the gaseous medium that surrounds it. Convection has been modeled classically using the following relationship generally attributed to Isaac Newton:

$$q_c = \bar{h}_c A(T_\infty - T_s) \tag{4}$$

where q_c is the rate of energy transferred attributable to convection (calories/s), T_s the exposed solid surface temperature (°C), T_∞ the fluid temperature far away from the exposed solid surface (°C), A the transfer area (cm^2), and $\bar{h}_c$ is the average convective heat transfer coefficient (calories/s cm^2 °C).

The apparent simplicity of Eq. 4 can be misleading, because the convective heat transfer coefficient is actually a very complex function of fluid flow conditions, fluid properties, and system geometry. In addition, the fluid flow patterns are significantly different depending on whether or not the fluid motion is induced by buoyancy forces alone (termed natural or free convection), or generated by external mechanical means using pumps or blowers (termed forced convection). When a heated fluid passes over a solid surface, the regions of significant velocity and temperature change are generally restricted to a small layer in the immediate vicinity of the solid surface. This boundary layer may consist entirely of fluid moving in the laminar flow regime, where transport of both momentum and energy rely solely on molecular interactions. More generally, the boundary layer consists of both a laminar sublayer immediately adjacent to the solid surface and a turbulent region.

Classical techniques have relied heavily on dimensional analysis (3), the combining of the many variables into physically meaningful nondimensional groups, supported with experiments to quantify heat transfer for various geometries. For most drying applications of pharmaceutical relevance, the most important of these nondimensional groups are the Nusselt number ($\overline{\mathrm{Nu}}$), the Prandtl number (Pr) and the Reynolds number (Re), defined as follows:

$$\overline{Nu} = \frac{\mathrm{h}L}{k_\mathrm{f}} \tag{5a}$$

$$Pr = \frac{c_p \mu}{k_\mathrm{f}} \tag{5b}$$

$$Re = \frac{VL\rho}{\mu} \tag{5c}$$

Here, k_f, c_p, ρ, and μ are, respectively, the thermal conductivity, specific heat at constant pressure, density, and dynamic viscosity of the convective fluid; V is the relative velocity between fluid and solid; and L is a geometry dependent, characteristic length dimension for the system. Note that the Pr is composed exclusively of fluid properties and that the Re will increase in direct proportion to the relative velocity between fluid and solid surface. Example applications are shown in Fig. 2.

Knowledge of $\overline{\mathrm{Nu}}$, fluid phase thermal conductivity, and characteristic length allows computation of the average convective heat transfer coefficient, using Eq. 5a. For flat surfaces, like the surfaces of static beds exposed to air or other gases ($Pr \approx 0.7$), Kreith (4) provides the following for low-velocity, laminar flow conditions

$$\begin{aligned} &\overline{Nu} = 0.664\, Re_\mathrm{L}^{0.5} Pr^{0.33} \\ &\text{for} \quad Pr > 0.1 \\ &\text{and} \quad Re_\mathrm{L} < 5 \times 10^5 \end{aligned} \tag{6a}$$

and for high-velocity, turbulent conditions

$$\begin{aligned} &\overline{Nu} = 0.036\, Pr^{0.33} [Re_\mathrm{L}^{0.8} - 23,200] \\ &\text{for} \quad Pr > 0.5 \\ &\text{and} \quad Re_\mathrm{L} > 5 \times 10^5 \end{aligned} \tag{6b}$$

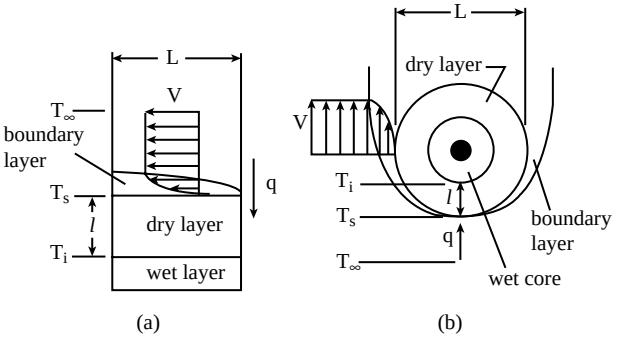

Fig. 2 Convective heat transfer applications in pharmaceutical drying: (a) tray-drying of a static solids bed; and (b) fluid bed-drying of a spherical particle.

For a spherical particle moving in an air or other gaseous stream, Whitaker (5) recommends the following relationship:

$$\overline{Nu} = 2 + (0.4Re_L^{0.5} + 0.06Re_L^{0.67})Pr^{0.4}(\mu_s/\mu_\infty)^{0.25} \quad \text{for } 3.5 < Re_L < 76{,}000 \tag{6c}$$

where μ_s and μ_∞ are the dynamic viscosities of the gas at the temperature of the particle surface and at the temperature far away from the surface, respectively. In the limiting case of $Re_L \ll 1$, Johnston et al. (6) have shown that the $\overline{Nu}$ approaches the constant value of 2, using assumptions approximating spherical particles in gas streams.

Equipment designs based on indirect conduction usually transfer the heat from the primary heat transfer fluid to the intermediate wall within some kind of internal duct or channel. Transfer coefficients for these cases depend on the nature of the flow (laminar or turbulent) and the geometry of the duct or channel (short or long). Expressions for evaluating the transfer coefficients for these cases are available in standard texts (7).

An expression for the convective thermal resistance can be generated similar to that derived for the conductive resistance:

$$q_c = \frac{(T_\infty - T_s)}{R_c} \tag{7}$$

Here, $R_c = \frac{1}{\bar{h}_c A}$, is the convective thermal resistance.

The third mechanism of heat transfer is thermal radiation that can be defined as radiant energy emitted by a medium by virtue of its temperature. The wavelengths of thermal radiation produced by emitting bodies fall roughly between 0.1 and 100 μm, which includes portions of the ultraviolet, visible, and infrared spectra. The net exchange of radiant thermal energy between two surfaces can be characterized by the following relationship

$$q_r = \sigma A_1 \Im_{1\text{–}2}(T_1^4 - T_2^4) \tag{8}$$

where q_r is the rate of energy transferred attributable to thermal radiation (calories/s), T_1 the absolute temperature of radiating surface 1 (K), T_2 the absolute temperature of radiating surface 2 (K), σ the Stefan–Boltzmann constant (1.35×10^{-12} cal/s cm^2 K^4), A_1 the transfer area of surface 1 (cm^2), and $\Im_{1-2}$ is a dimensionless factor that corrects for the radiative properties and relative geometries of the surfaces involved in the exchange.

Most of the complexity of radiative heat transfer analysis is thus condensed into evaluation of the dimensionless factor $\Im_{1-2}$. This factor is a function of both surface properties and the geometric orientation of the surfaces involved in the exchange. For real surfaces the amount of thermal radiation emitted and absorbed depends on the temperature, the wavelength, and the angular direction. These complications are often neglected and the radiative properties of the surface are lumped together into a dimensionless factor that is independent of both wavelength and direction, referred to as emissivity (ε). The emissivity expresses the radiative power of a surface as some fraction of an ideal radiator or blackbody. Real surfaces so treated are referred to as greybodies to emphasis this simplification imposed. For exchanges between parallel rectangular surfaces, where the spacing between the surfaces is small compared with the smaller dimension of the rectangles, the factor $\Im_{1-2}$ can be estimated as

$$Im_{1\text{–}2} = \frac{1}{\frac{1}{\varepsilon_1} + \frac{1}{\varepsilon_2} - 1} \tag{9}$$

where, ε_1, ε_2 are the emissivities of the surfaces involved in the exchange. For a small spherical particle inside a large enclosure, the factor $\Im_{1-2}$ can be estimated as

$$\Im_{1\text{–}2} = \varepsilon_1 \tag{10}$$

where ε_1 is the emissivity of the spherical particle. For more rigorous treatments, the reader is advised to consult advanced texts (8). Eq. 8 can be used to generate an expression for the thermal radiative resistance similar to that derived for the conductive and convective resistance:

$$q_r = \frac{(T_\infty - T_s)}{R_r} \tag{11}$$

Here the thermal radiative resistance must assume a more complex form

$$R_r = \frac{(T_\infty - T_s)}{\sigma A_s \Im_{s\text{–}2}(T_2^4 - T_s^4)} \tag{12}$$

with the subscripts s and 2 used to denote the product surface and external radiating surface, respectively.

Unfortunately, the resistance defined by Eq. 12 cannot be evaluated without a priori knowledge of temperatures, unlike those defined previously for conduction and convection. However, enough information on temperatures is often available from previous drying experience to permit useful estimates of the radiative resistance to be established.

Application of the Ohm'–s law analogy allows construction of combined series parallel thermal circuits to describe a specific drying application. The flow of heat energy through the circuit shown in Fig. 3 can be described as

$$q = \frac{(T_\infty - T_i)}{R_T} \tag{13}$$

where

$$R_T = R_k + \frac{R_c R_r}{(R_c + R_r)} \tag{14}$$

is the total resistance to heat transfer for the circuit. If $R_r \gg R_c$ then the radiation transfer mode can be neglected and the total resistance simplifies to

$$R_T = R_k + R_c \tag{15}$$

In the early stages of the drying operation, the thermal resistance attributable to conduction through the dried layer will be negligibly small for the cases illustrated in Figs. 1a and c because the thickness ℓ will approximate zero. For this early stage, the thermal resistance would be

$$R_T = \frac{R_c R_r}{(R_c + R_r)} \tag{16}$$

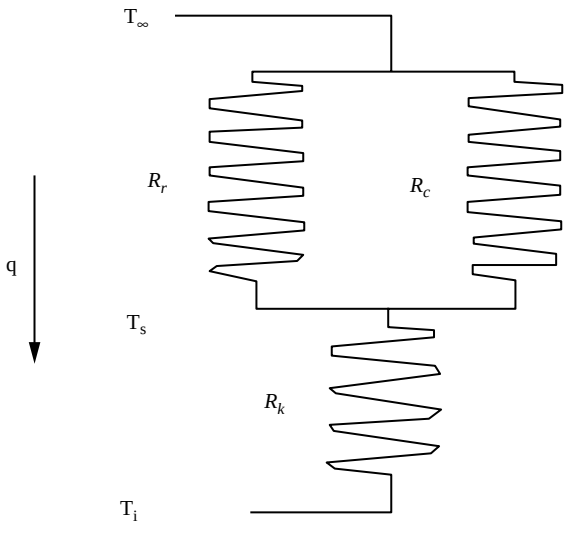

Fig. 3 Construction of a thermal circuit for a drying application.

or

$$R_T = R_c \tag{17}$$

depending on whether or not thermal radiation is appreciable. For a fixed temperature difference and flow rate, we would then expect to generate a constant heat transfer rate during this initial drying period, since the parameters that make up R_T using either Eq. 16 or Eq. 17 are at most dependent on fluid velocity and temperature. As drying proceeds we will expect the thermal resistance attributable to conduction through the growing dried layer to increase and eventually become a significant part of the total resistance. If temperature and flow conditions are fixed, we would therefore expect a decrease in heat transfer rate with time. Heat will continue to flow as long as there is a temperature difference between the energy source and the product.

Mass Transfer

The vapor generated during drying must migrate from the liquid vapor interface through the dried material layer and then be transported out of the drying equipment. For purely diffusional transport, exact solutions to Fick'–s law are available for a variety of geometric configurations and boundary conditions, usually in the form of infinite series. For a layer of wet material drying off the top surface from an initial uniform concentration of c_0 with the top surface maintained at a constant concentration of c_1 the drying rate for a purely diffusion based-based transfer mechanism is (9)

$$\dot{m} = \frac{2D(c_0 - c_1)}{\ell} \sum_{n=0}^{\infty} \exp\left[\frac{-(2n+1)^2 \pi^2 D t}{4\ell^2}\right] \tag{18}$$

where m is the rate of vapor transferred by the diffusion mechanism (g/s), D the mass diffusivity of the dried layer (cm^2/s), A the transfer area, (cm^2) ℓ the layer thickness (cm), and t the elapsed time (s).

Eq. 18 leads to the following expression for the expected drying curve

$$\frac{M(t)}{M_0} = \frac{8}{\pi^2} \sum_{n=0}^{\infty} \frac{1}{(2n+1)^2} \exp\left[\frac{-(2n+1)^2 \pi^2 D t}{4\ell^2}\right] \tag{19}$$

where $M(t)$ is the amount of solvent in the dried material at time t(g), and M_0 is the initial amount of removable solvent (g).

The corresponding expressions for the drying rate and drying curve of a spherical particle from an initial uniform concentration of c_0 with the exposed surface maintained at a constant concentration of c_1 are (10)

$$\dot{m} = 8Dr_0\pi(c_0 - c_1)\sum_{n=1}^{\infty}\exp\left[\frac{-n^2\pi^2Dt}{r_0^2}\right] \tag{20}$$

and

$$\frac{M(t)}{M_0} = \frac{6}{\pi^2}\sum_{n=1}^{\infty}\frac{1}{n^2}\exp\left[\frac{-n^2\pi^2Dt}{r_0^2}\right]. \tag{21}$$

where r_0 is the particle radius. Expressions such as Eqs. 18 and 20 illustrate the role of concentration difference as the driving force behind mass transfer and predict a decrease in drying rate with time. However, these expressions tend to overstate the magnitude of the decrease and the dependence on layer thickness and/or particle radius (11).

The total mass transferred will include the combined effect from a number of mechanisms, including molecular diffusion through the solid via vacancies and interstitial defects, migration along dislocations, grain boundaries, and along surfaces of internal pores and fissures, and molecular diffusion through the vapor filled passages defined by the internal pores and fissures (12, 13). In cases where the total pressure inside the material is higher than ambient, the transport mechanism could include convective flow through the pores and fissures.

The two-zone model described above allows for the multiple mechanisms. The rules that govern these mass transfer operations are completely analogous to those governing heat transfer already discussed. The migration of vapor through the dried material layer can be expressed as

$$\dot{m} = -D_{\text{eff}}A\frac{\mathrm{d}c}{\mathrm{d}x} \tag{22}$$

where $\frac{\mathrm{d}c}{\mathrm{d}x}$ is the concentration gradient in the direction of transfer (g/cm^3/cm). The effective mass diffusivity (D_{eff}) will include the combined effect from all the mechanisms outlined above.

Eq. 22 can be recast using vapor phase pressure as the driving force behind the mass transfer, using the ideal gas relationship,

$$\dot{m} = -D_{\text{eff}}A\left(\frac{\text{MW}_s}{\bar{R}T}\right)\frac{\mathrm{d}p}{\mathrm{d}x} \tag{23}$$

where MW_s is the molecular weight of the solvent (g/mole), $\bar{R}$ the molar gas constant (62364.1 mm Hg cm^3/mole K) and T is the absolute temperature (°K).

Using appropriate simplifying assumptions, Eq. 23 can be integrated and placed in a form analogous to Eq. 3

$$\dot{m} = \frac{(p_s - p_i)}{\Re_D} \tag{24}$$

where p_s, p_i are the vapor pressures at the exposed surface and interface, respectively (mm Hg), and

$$\Re_D = \frac{\ell}{D_{\text{eff}}A}\left(\frac{\overline{R}T}{\text{MW}_s}\right)\left(\frac{p_m}{P}\right) \tag{25}$$

is the effective mass transfer resistance of the dried layer (mm Hg s/g). Here P is the total pressure and

$$p_m = \frac{(p_s - p_i)}{\ln\left(\frac{P - p_i}{P - p_s}\right)} \tag{26}$$

referred to as the logarithmic mean partial pressure, accounts for the fact that the partial pressures of the individual components in a multicomponent system must equal the system'–s total pressure. For dilute mixtures of solvent vapor in air, $p_m \cong P$ and the pressure ratio on the right-hand side of Eq. 25 approximates 1.

Solvent transfer from the surface of the dried material can be treated in a manner analogous to Eq. 4 above for heat transfer. An expression for the convective mass resistance can be generated similar to that derived for the thermal resistance:

$$\dot{m} = \frac{(p_\infty - p_s)}{\Re_c} \tag{27}$$

Here, $\Re_c = \frac{1}{\overline{h}_G A}$, is the convective mass resistance (mm Hg s/g), $\dot{m}$ = the rate of vapor transferred from the exposed surface (g/sec), p_s = the partial pressure of solvent at the exposed solid surface temperature (mm Hg), p_∞ = the partial pressure of solvent far away from the exposed solid surface (mm Hg), A = the transfer area (cm^2), and $\overline{h}_G$ = the average convective mass transfer coefficient (g/s-cm^2-mm Hg).

Convective mass transfer coefficients must generally be determined by experiment. Again dimensional analysis can be used to determine physically meaningful nondimensional groups to guide experimental designs. For most drying applications of pharmaceutical relevance, the most important of these nondimensional groups are the Sherwood number (*Sh*), the Schmidt number (*Sc*), and the Reynolds number (*Re*). The *Sh* and *Sc* are defined as follows:

$$Sh = \frac{\overline{h}_G L}{D_v}\left(\frac{\overline{R}T}{\text{MW}_s}\right)\left(\frac{p_m}{P}\right) \tag{28a}$$

$$Sc = \frac{\mu}{D_v\rho} \tag{28b}$$

Here, D_v is the mass diffusivity of the solvent through the convective fluid and all other parameters are as defined previously.

The powerful analogy that exists among momentum, heat, and mass transport permits useful values of convective mass transfer coefficients to be calculated from known values of convective heat transfer coefficients. For a particular drying system with a specific geometry and flow characteristics, the following relationship is recommended (14).

$$\overline{h}_G = \left(\frac{\overline{h}_c}{c_p \rho}\right)\left(\frac{MW_s}{\overline{R}T}\right)\left(\frac{P}{p_m}\right)\left(\frac{Pr}{Sc}\right)^{0.67} \tag{29}$$

Once again, application of the Ohm'–s law analogy allows construction of mass transfer circuits to describe a specific drying application. The mass flow through the circuits derived from Fig. 2 can be described using

$$\dot{m} = \frac{(p_i - p_\infty)}{\Re_T} \tag{30}$$

where

$$\Re_T = \Re_D + \Re_c \tag{31}$$

The mass transfer resistance of the dried layer will be negligibly small for some period at the start of drying because the dried layer thickness, starts at zero. During this period the total resistance to mass transfer will equal the convective resistance. For fixed flow, temperature, and solvent concentration far from the exposed product surfaces, the drying rate will be constant during this period. As drying proceeds the resistance of the dried layer becomes a significant portion of the total resistance and continues to increase with time. The drying rate would steadily decrease during this period even if the solvent pressure difference could be held constant.

Phase Transition

The liquid solvent added to a pharmaceutical material generally exists in a variety of states (15). Some will condense or be pulled by capillary forces into macroscopic pores and fissures or into the interstitial spaces between particles. A state of local equilibrium can be assumed to exist at the interface between the liquid and vapor phases of solvent so situated. As a result, the temperature and vapor pressure exerted by the condensed solvent will not be independent of one another. Fig. 4 shows the equilibrium vapor pressure versus temperature relationship for a number of common solvents (16). Heats of vaporization are shown parenthetically (17). Among common solvents, acetone has the highest vapor pressure and water the lowest. Water requires three–five times the energy of the common organic solvents to vaporize.

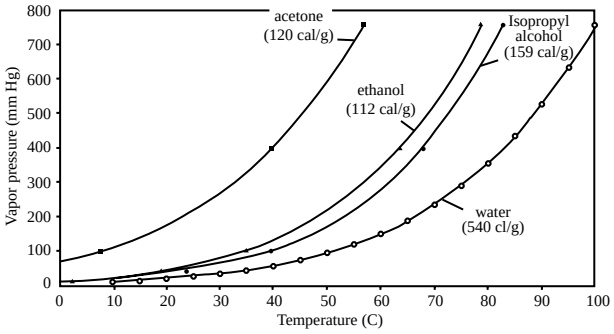

Fig. 4 Vapor pressure curves for common solvents. Heats of vaporization are shown parenthetically. (From Refs. 16 and 17.)

Some of the solvent added will adsorb to the solid surfaces of crystalline solids, particularly at higher energy sites resulting from surface defects and impurities. The amount adsorbed will increase in proportion to the exposed surface area and as the partial pressure of solvent vapor above the surface increases. Solvent can also concentrate in the crystal interior by migrating along high-diffusion paths produced by dislocations and grain boundaries (18). Some polymeric materials of pharmaceutical interest, such as starches and celluloses, often exhibit noncrystalline or amorphous structures. Such materials will typically take up solvent in significantly greater quantities than do crystalline materials with the amount absorbed independent of surface area. As with crystalline solids the amount sorbed will increase as the partial pressure of solvent vapor in contact with the material increases. Sorption data can be experimentally generated and fitted to a variety of available models, including the well-known BET equation, and the more generally applicable 3-state extension developed by deBoer and Guggenhein (19). Data on a number of relevant pharmaceutical materials have been compiled by Callahan and collaborators (20).

In some cases the water or organic solvent added move to regular positions in the crystal lattice and form a stoichiometric relationship with the original molecules resulting in a hydrate or solvate crystalline structure that differs from that of the original crystalline material. Solid state techniques, such as X-ray diffraction, can be used to detect these structural changes. For these materials the impact of solvent addition and removal through drying must be carefully considered as new states with unknown or undesirable properties could be inadvertently generated. In the case of erythromycin, researchers have reported that the method of removing the water of hydration leads to a collapse of the crystalline structure into a metastable amorphous form (21). On the other hand, Schilling and coworkers monitored the formation of a hydrated form of a

5-lipoxaginase inhibitor during wet granulation and subsequent return to the desired anhydrous state after fluid bed-drying (22).

The energy that flows to the water or organic solvent interface is used in two ways. First, and most desirable, it is used to transform the water or organic solvent from a liquid or liquid-like state to a vapor state. The second use, often less desirable, is to raise the temperature of the interface. The distribution can be expressed in terms of an energy balance

$$q_t = \dot{m}\Delta h + Mc_p \frac{(T_i' - T_i)}{\Delta t} \tag{32}$$

where q_t is the total rate of energy transferred to the interface from all sources and mechanisms (calories/s), Δt the time interval under consideration (s), T_i' the temperature of the interface at the end of the time interval (°C), T_i the temperature of the interface at the beginning of the time interval (°C), Δh the solvent'–s heat of vaporization (calories/g), M the effective mass of wet product associated with the interface (g), c_p the heat capacity of the wet product (calories/g°C), and $\dot{m}$ is the drying rate (g/s).

Eq. 32 can be used to understand the link between drying rate, heat flow, and temperature rise during drying. If the resistance to mass transfer is sufficiently low so solvent vapor molecules generated at the interface can freely escape from the solid, then the bulk of the energy supplied will be absorbed by the first term on the right-hand side of Eq. 32 and the interface will remain cool. This is generally the case near the beginning of the drying cycle because the mass transfer barrier created by a dried product layer has not yet formed. The rate of energy transferred is generally fixed by inlet temperature and flow conditions, leading to a constant drying rate. This portion of the drying cycle is referred to as the constant rate period. As the dried product layer builds the vapor molecules generated cannot readily escape, causing the vapor pressure at the interface to increase. Because temperature and pressure at the interface are related through the equilibrium relationship, the interface temperature increases as the vapor pressure increases. More and more of the energy supplied then shifts from the first to the second term on the right-hand side of Eq. 32 resulting in a drop in the drying rate and a product temperature rise during the time interval. This portion of the drying cycle is referred to as the falling rate period. The higher interface temperature and higher heat transfer resistance created by the dried product barrier serve to reduce the rate of energy transfer in subsequent time intervals as predicted by Eq. 13. The higher interface pressure partially offsets the effect of increasing the mass transfer resistance.

Psychrometrics

The solvent vapor generated during drying must be transported out of the drying equipment. If it isn'–t, the gas surrounding the material to be dried will soon become saturated with vapor and drying will cease. Various interconvertible terms have evolved over time to express the amount of solvent that is absorbed by the drying gas. Many of the common terms have been defined strictly to apply to the air–water vapor system. However, the concepts involved apply equally well to any solvent–drying gas combination. The most common term is that of relative humidity (ϕ), which expresses the ratio of the actual amount of water vapor present to the maximum amount that could be present at a specified temperature. Amounts can be expressed in any consistent way, including units of mass, moles, or partial pressures. For drying applications, partial pressures are particularly convenient and the relative humidity becomes

$$\phi = \frac{p_\infty}{p_{sat}} \tag{33}$$

where p_∞ is the partial pressure of solvent vapor present and p_{sat} is the maximum pressure at saturation. The saturation pressures for common solvents have been shown previously (Fig. 4) as a function of temperature. For ease of computation, saturation data can be fit to an equation of the form

$$\ln(p_{sat}) = A + \frac{B}{T} + C\ln(T) + DT \tag{34}$$

where T is the absolute temperature and the constants A, B, C, and D depend on the solvent (23). Recommended constants for the common solvents, determined through regression, are listed in Table 1 for p_{sat} in mm Hg and temperature expressed in K.

An alternate expression for solvent content is the specific humidity or humidity ratio, which is defined as the ratio of the mass of solvent vapor present to the mass of dry gas

$$\omega = \frac{m_v}{m_g} = \left(\frac{MW_v}{MW_g}\right)\left(\frac{P_v}{P_g}\right) \tag{35}$$

Eqs. 33, 34, 35 allow interconversion from one expression for solvent content to another. For example, knowledge of temperature, total pressure, and relative humidity allows the humidity ratio to be determined using

$$\omega = \left(\frac{MW_v}{MW_g}\right)\left(\frac{\phi P_{sat}}{P - \phi P_{sat}}\right) \tag{36}$$

Solvent content can be portrayed graphically in what is known as a psychrometric chart, such as the one for an air

Table 1 Recommended constants for computing saturation pressure, using Eq. 34 for common solvents (p_{sat} in mm Hg and T in K)

Solvent	A	B	C	D
Water	70.708779	−7175.9470	−7.9064596	0.0053125111
Ethanol	−93.710636	−2458.5969	20.649371	−0.039031369
Isopropyl alcohol	−7.4598754	−5.017.1464	5.7374144	−0.015489516
Acetone	92.141422	−6280.1292	−12.241911	0.013701258

water system at atmospheric pressure shown in Fig. 5. Such a chart is a convenient tool for converting between the different expressions for solvent content and for tracking changes in solvent content during drying. Say, for example, that drying air enters a dryer at 60°C and a relative humidity of 0.05 (point A in Fig. 5) and leaves at 30°C and a relative humidity of 0.90 (point B in Fig. 5). Moving horizontally and to the left from point A shows the inlet condition corresponds to a moisture vapor pressure of approximately 7.5 mm Hg and by moving horizontally and to the right shows a humidity ratio of approximately 0.006. The exit condition (point B in Fig. 5) corresponds to a humidity ratio of 0.024 for a difference of approximately 0.018 g of water vapor carried out of the system per gram of dry air. The intersection of the moisture content (horizontal) lines with the saturation curve ($\phi = 1.0$) uniquely defines the so called dew point temperature, indicated in Fig. 5, which is yet another way of specifying solvent content. Fig. 5 can also be used to illustrate the effect of product temperature on the mass transfer driving force. For example, product at 17.5°C (point C in Fig. 5) would provide a driving force of approximately 7.5 mm Hg (15.0–7.5 mm Hg) between the solvent vapor interface and the inlet drying air. A modest temperature rise to 24°C approximately doubles the driving force with the same inlet air by increasing the vapor pressure at the solvent vapor interface.

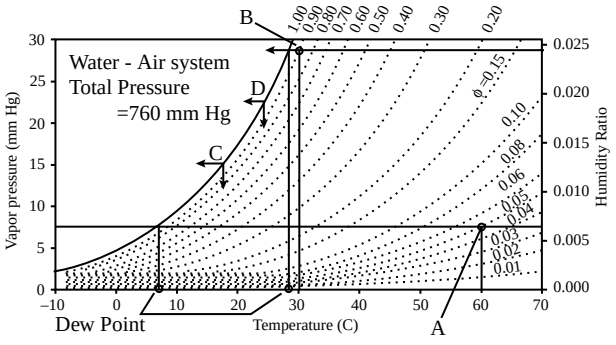

Fig. 5 Psychrometric chart for an air–water system at a total pressure of 760 mm Hg.

PRACTICE

Drying can be carried out successfully using a variety of commercially available equipment designs. Pharmaceutical drying equipment has been classified according to principal mode of operation in a recently published regulatory guidance document (24) as shown in Table 2. Equipment classified as direct heating allows intimate contact between the material being dried and the heat energy source, usually a heated gas. That same gas is used to transport the vapor generated from the equipment. In indirect conduction, the energy is transferred from the source, usually a heated liquid, to the material being dried through a conducting wall. In this case other means must be used to remove the generated vapor from the equipment. Radiant approaches do not rely on temperature to generate or transfer the needed energy to the material being dried. Instead, the material is exposed to electromagnetic energy at frequencies strongly absorbed by the solvent being targeted for removal. Specialized approaches, such as spray drying and lyophilization, are treated in separate articles in this encyclopedia and will not be covered more here.

Tray and Truck-Drying

Historically, the most common method of drying of pharmaceutical powders has been tray-drying. With this method, wet powder or granulation is placed on paper-lined trays, usually solid or perforated metal, which are then placed directly onto racks in a drying chamber (oven) or onto movable racks, or trucks, that are wheeled into an oven. The heat and low relative vapor pressure of solvent provided by the flow of heated, dry air throughout the chamber provide a driving force for solvent transfer to and subsequent removal from the particle surfaces of the powder. This results in the gradual overall loss of solvent from the bulk powder.

The drying process from solids has been characterized by three drying regions, as shown in Fig. 6 (12, 25). The

Table 2 Classification of pharmaceutical drying equipment

Class	Subclass	Common names
Direct heating	Static solids bed	Tray and truck dryers
	Moving solids bed	Belt dryer
	Fluidized solids bed	Fluid bed dryer
	Dilute solids bed	Spray dryer
Indirect conduction	Moving solids bed	Tumble dryer
	Gas stripping	Zanchetta
	Static solids bed	Heated shelf tray drier
	Lyophilizers	Freeze dryer
Radiant	Microwave, moving solids bed	Microwave dryer

first, termed the Constant Rate Period, is the initial drying phase in which surface moisture exceeds a critical level and rate is controlled by surface area. When the level of moisture falls below the critical level, it begins to be controlled by mass transfer from inside the solid mass: this is called the First Falling Rate Period. As drying proceeds, mass transfer is not able to supply moisture to the surface of the solid mass at a rate equal to the drying rate, and the free water content at the surface goes to zero. At this time, the surface temperature rises rapidly, and a receding evaporation front may be formed that divides the solid into a wet region and a dry or sorption region. This is the beginning of the Second Falling Rate Period, during which mass transfer of moisture vapor through the sorption region becomes more and more retarded.

The falling rate portion of the drying process can be generally modeled by using a variation of Eq. 19 in which the summation is truncated after one term:

$$\ln\left(\frac{M(t)}{M_0}\right) = -\left(\frac{\pi^2 D}{4\ell^2}\right)t + \ln\left(\frac{8}{\pi^2}\right) \tag{37}$$

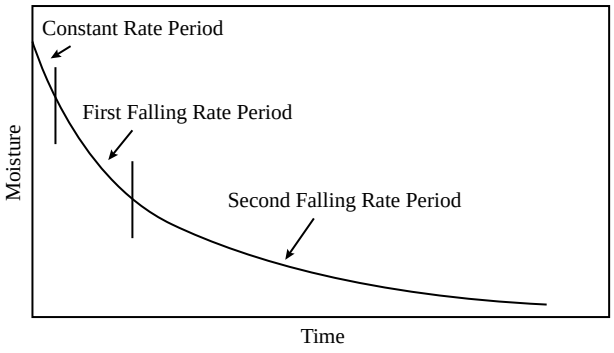

Fig. 6 The phases of the drying process. (From Ref. 12.)

Eq. 37 can be simplified to

$$\ln\left(\frac{M(t)}{M_0}\right) = -kt - 0.2 \tag{38}$$

where k is a first-order drying rate constant such that when $\ln(M(t)/M_0)$ is plotted versus time a straight-line relationship is obtained with a slope of $-k$ (11). This becomes very useful in trying to model the tray-drying process and evaluating the impact of process variables such as bed thickness and drying temperature changes. An example of this is given in Fig. 7, in which drying rate constants obtained at multiple temperatures are plotted versus inverse temperature, allowing one to predict drying rate at any interpolated temperature.

During the drying process, internal liquid transport occurs via capillary flow, while vapor transport occurs both via diffusion and true mass flow driven by pressure gradients (12, 26). Because the powder bed is static,

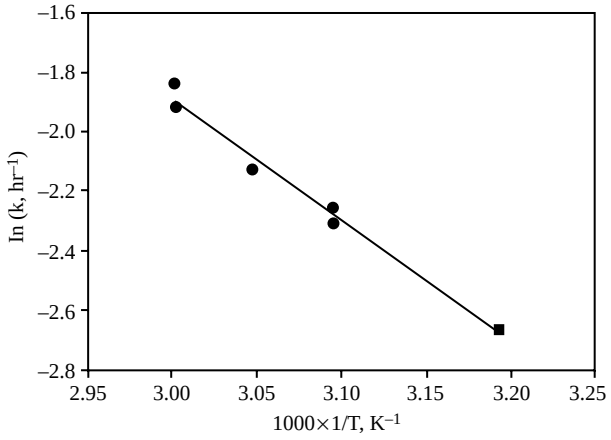

Fig. 7 Temperature dependence of drying rate constant (k from Eq. 38). (From Ref. 11.)

significant resistance to the diffusion of solvent from the bed as a whole reduces the rate of drying, thereby limiting the efficiency of this method of drying. This is demonstrated by the dependence of the first order rate constant k on the depth of the bed being dried. Theoretically it is shown that the drying rate constant is an inverse function of the square of the bed thickness (see Eq. 37), but experimental data shows a relationship that more closely resembles an inverse relationship of k with the first order of bed depth (11).

Tray-drying is also used as a method to remove water from soft elastic gelatin capsules (27), and can be model according to Eq. 39a:

$$\ln(c - c_\infty) = -\frac{t}{\Gamma} + \ln(c_0 - c_\infty) \tag{39a}$$

where

$$\Gamma = \frac{h^2}{5.8D} \tag{39b}$$

Here c is the amount of moisture at time t, c_0, c_∞ the amounts of moisture at time zero and infinity, respectively, h the thickness of the gelatin film, and D is the diffusion coefficient of moisture through gelatin.

This modeling becomes important as a soft-gel product is being developed and a drying end point needs to be established and reproduced.

Despite the low relative capital investment required for tray-drying, it provides a low rate of drying and the loading and unloading of trays is a labor-intensive process. Although still commonly found in both drug substance and drug product manufacturing procedures, tray-drying has become less popular in comparison to other more efficient, reproducible, and well-defined drying procedures such as fluid bed and vacuum tumble drying.

Fluid Bed Dryers

Fluid bed-drying is a widely used example of the direct heating classification. Drying is accomplished by suspending the particles to be dried directly in a stream of heated air or other gaseous media. The intimate contact and high surface areas available for transfer result in fast, efficient drying, often making fluid bed the approach of choice for high-volume products.

A typical installation is shown in Fig. 8. Ambient air enters an air-handling unit through a coarse filter in the lower right. The air is first passed over a chilled, condensing coil to reduce the moisture content. The air leaving the coils can be assumed to be in equilibrium with the condensed water so the temperature measured at the coil outlet represents the wet bulb temperature, a measure of moisture content. The coolant temperature determines the degree of dehumidification achieved. Chilled water and refrigerant are common coolants. A portion of the inlet air is then diverted through louvers past a heat source and then allowed to remix with the portion not diverted. A steam coil is commonly used as the heat source. The louvers are mechanically linked so that one flow path opens as the other closes. A feedback loop can be established between the downstream temperature and the louver position to control drying temperature. If the drying temperature drops below the set point, the louver position is adjusted to divert a larger fraction of the incoming airflow past the heat source, resulting in a higher temperature of the remixed streams. If the drying temperature drifts above the set point, the louvers are repositioned to divert less past the heat source. This type of arrangement is referred to as *face and bypass* control and has the advantage of fast response time and minimal overshoot. The warm, dehumidified air is then passed through a second, finer filter and sent to the dryer.

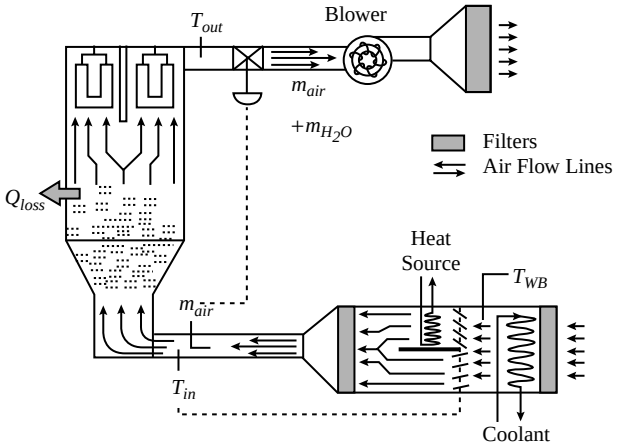

Fig. 8 Schematic of a typical fluid bed dryer installation.

The product to be dried is placed inside a bowl on top of a retaining screen. The retaining screen can be of the wire mesh, perforated plate, gill plate, or combination design. As the drying air enters the bowl from below, it drags the product particles off the retaining screen and entrains them in the flow stream. The air transfers heat energy to the suspended particles and collects the solvent vapors given off. A small part of the heat energy supplied to the drying air stream is lost through transfer to the surrounding environment. Product filters are provided to prevent the entrained particles from leaving the drying chamber. A split filter design allows for periodic cleaning without disrupting the drying operation. Flow through one filter

segment can be interrupted so it can be mechanically shaken or reverse-pulsed with clean air to remove accumulated particles. Flow then resumes and the cleaning operation is performed on the other segment.

Drying air flow rate control is achieved using a blower that works against a flow control valve. Both are typically located on the downstream side of the drier to maintain the drying chamber at a slight but not excessive negative pressure with respect to ambient. Product particles and organic solvent vapors are thus unable to escape against the negative pressure gradient. The airflow rate is measured, usually on the clean and dry upstream side of the drier, and a feedback loop is established with the flow control valve. Flow control is achieved by adjusting the position of the flow control valve. Before releasing the used air back into the environment, it is filtered once more to remove any pharmacologically active and potentially hazardous product particles that may have leaked past the product filters. For organic vapor applications, the spent air would also be treated to separate and remove the vapors from the air stream before releasing it back to the environment. Grounding, containment, and venting strategies are incorporated into the designs to control explosion hazards.

The dryer bowl is designed in the shape of an inverted frustum of a right circular cone, with the smaller diameter at the bottom of the bowl. As the drying air passes up through the bowl, the increasing area causes the flow velocity to drop in the direction of flow. At the lower velocity the larger, heavier particles can no longer be sustained and they fall back toward the retaining screen. The situation represents a tension between the drag forces exerted on the particle by the moving fluid and the force of gravity trying to pull the particle back down to the retaining screen. For spherical particles moving at low velocity in a fluid stream the expression for the drag force first determined by Stokes (28) can be set equal to the particle weight to yield an expression for the minimum fluidization velocity (29)

$$V = \frac{gd^2}{18\mu}(\rho_p - \rho) \tag{40}$$

where V is the minimum fluidization velocity (cm/s), d the particle diameter (cm), g the acceleration of gravity (980 cm/s^2), ρ_p the particle density (g/cm^3), and ρ and μ are the density and dynamic viscosity of the fluid, respectively.

Strictly speaking, Eq. 40 is a good approximation only at low *Re*, that is at particle diameters significantly less than 0.01 cm (100 micrometers). White (30) has provided a formula extending the range to particle diameters as high as 1 cm, using a curve fit of data from many sources. A plot

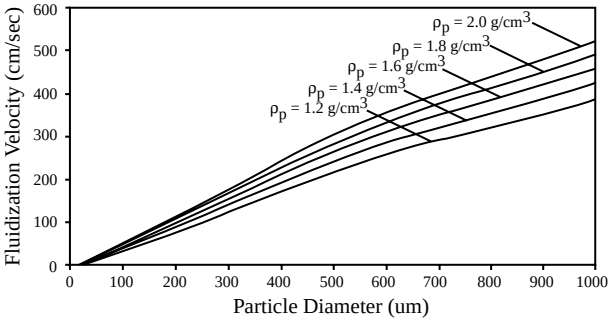

Fig. 9 Fluidization velocity as a function of diameter and density for spherical particles suspended in an air stream at 45°C, using the curve fit of White. (From Ref. 30.)

of fluidization velocity as a function of particle diameter (in microns) and density is shown in Fig. 9 assuming spherical particles in air at 45°C, using White'–s formula. Typical commercial equipment provides velocities in the range of 150–250 cm/s at the retaining screen that drop after expansion into the range of 60–100 cm/s. Because particle density drops as drying proceeds, flow rates used at the beginning of drying to fluidize the particle bed could be reduced later in the cycle without losing entrainment.

The drying rate at any point in the drying cycle can be derived from information provided from available process instrumentation without resorting to intrusive sampling during the process. An energy balance across a control volume surrounding the drying bed yields:

$$\dot{m} = \frac{\dot{m}_g C_{p,g}(T_{in} - T_{out}) - Q_{loss}}{h_{fg}} \tag{41}$$

where $\dot{m}$ is the drying rate, $C_{p,g}$ the specific heat capacity of drying gas at constant pressure, $\dot{m}_g$ the mass flow of drying gas through dryer, T_{in} the inlet temperature of dryer gas, T_{out} the outlet temperature of dryer gas, Q_{loss} the heat loss to the environment through thermal convection, and h_{fg} is the latent heat of vaporization for solvent.

The heat loss term can be estimated by applying Eq. 41 to conditions near the end of the drying cycle, where the evaporation rate is negligible.

$$Q_{loss} = \left[m_g C_{p,g}(T_{in} - T_{out})\right]_{\text{end of cycle}} \tag{42}$$

Using these conditions, the $\overline{h}A$ term is then calculated from the following equation and is assumed constant throughout the drying cycle:

$$Q_{loss} = \overline{h}A(\overline{T} - T_{amb}) \tag{43}$$

where $\overline{h}$ is the average convective heat transfer coefficient, A the external dryer surface available for heat transfer, $\overline{T}$

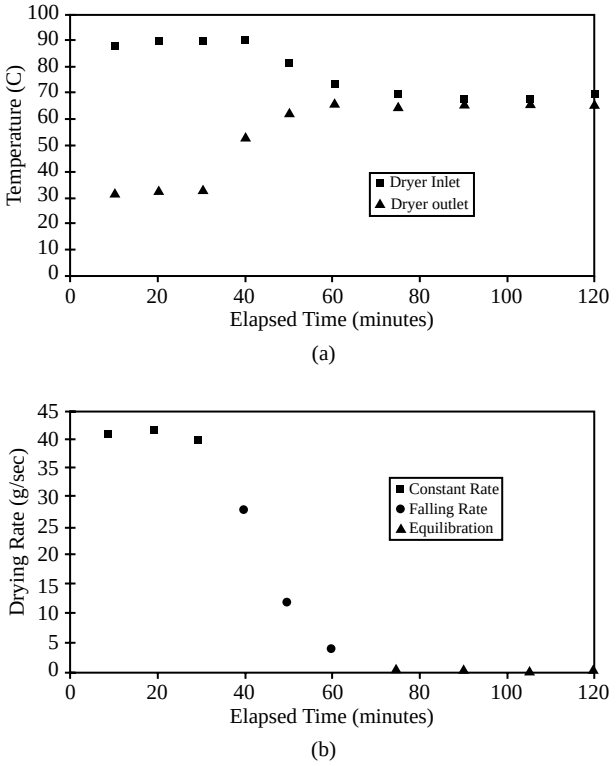

Fig. 10 Temperature and drying rate histories for a water-based drying case in air (a) temperature history; (b) computed drying rate history. (From Ref. 31.)

the average temperature in the drying bed, and T_{amb} is the ambient temperature.

The temperature and computed drying rate histories for a water based drying case in air at a constant flow rate of 2.36 $\times 10^6$ cm^3/s (5000 ft^3/min) is shown in Fig. 10 (31). The heat loss term parameter $\bar{h}A$ is computed to be 17.9 cal/s/°C for this case. An early constant rate period is evident that extends out to the first 30 min of drying in which a drying rate of approximately 40 g/s is achieved.

Because different mechanisms limit the drying rate in each of the drying periods, scheduled changes in flow rate and inlet temperature have been used with great success to shorten drying cycles without subjecting the pharmaceutical material to unnecessary stress (31, 32). During the constant rate period, the drying rate is limited by the enthalpy available in the inlet air and its capacity to absorb the vapor that is generated. Increases in flow rate and inlet temperature can be used to reduce the length of the constant rate period. Staged reductions in inlet temperature and flow rate can be scheduled without impacting the rate during the falling rate and equilibration periods because internal moisture transfer limits the overall rate. The lowest flow rates can be used during the equilibration period because the low-moisture, low-density particles are easiest to fluidize and because dehumidification techniques should become more efficient, resulting in inlet air with lower moisture content.

Vacuum Drying

Vacuum can be used with all of the indirect conduction and microwave approaches to drying. The total pressure surrounding the pharmaceutical material is reduced to levels below the saturation pressure of the solvent at the interface between the wet and dry layers causing generation of vapor. With suitable vacuum levels, drying can be cost-effective at relatively low product temperatures. Vacuum drying is particularly advantageous for heat- or oxygen-sensitive products, for reducing the risk of dust explosions, and for applications requiring solvent recovery or extremely low residual solvent levels.

A typical rotating double-cone vacuum dryer is shown in Fig. 11. Vapor exits the dryer via a tube that passes through a rotary seal along the axis of rotation. A filter prevents particles from leaving the dryer with the exiting vapor. Vacuum can be supplied by conventional pumps, blowers, or steam jets. Heating fluid circulates through a jacket and enters and exits through dynamic seals along the axis of rotation. Typical rotation speeds are 6–8 rpm. Working capacities, generally defined as 50% of total volume, range from 0.1 to 10 m^3 and vacuum levels range from just under ambient to 20 mm Hg (33). Indirect methods rely on contact between the wet material and the jacketed walls of the dryer to supply energy and the drying rate can be heat transfer-limited. Average drying rates range from 1–7 $kg/h/m^2$ of heat transfer surface area available. The ratio of jacket area to working volume tends

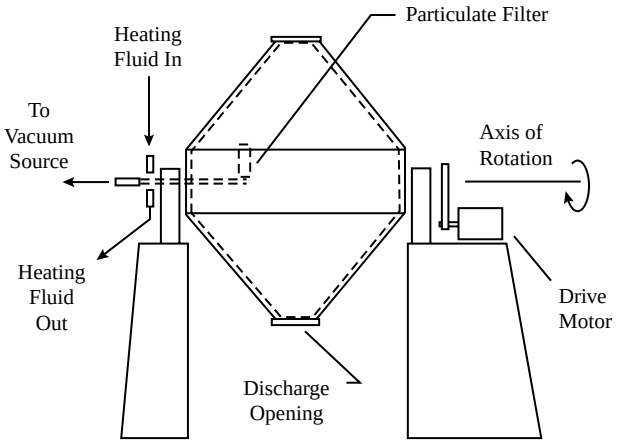

Fig. 11 Rotating double-cone vacuum dryer.

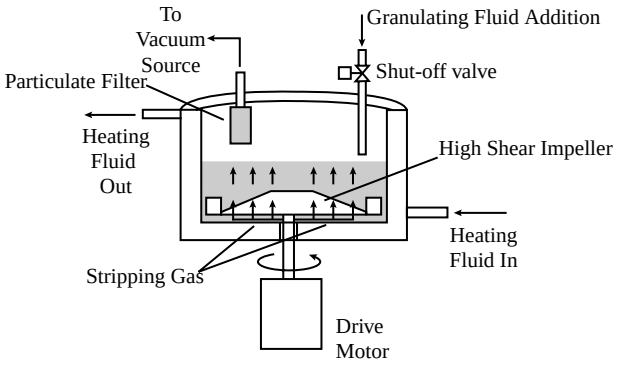

Fig. 12 High shear vacuum processor.

to decrease with increasing size, so larger models often require additional internal plates or pipe coils to increase available area for heat transfer (33).

Vacuum drying can be readily incorporated into high shear granulation designs to permit multiple processing steps to be completed in a single piece of equipment, as shown in Fig. 12. Granulation takes place in an initial processing step by introducing a fluid to the particle bed while mixing it with a high shear impeller. Vacuum drying follows. Typical vacuum conditions are 18–22 mm Hg. The vapor exits through a port in the cover through a tube equipped with a particulate filter. Heating fluid is circulated through the jacket of the bowl with typical operating temperatures of 60–80°C. Inert stripping gas (3–30 m^3/h depending of vessel volume) is introduced through the shaft seal to improve the convective transfer of vapor out of the vessel during drying. Gas stripping rates above an optimal level reduce the drying effectiveness by raising the pressure in the vessel. Commercial designs allow for tilting of the unit up through 180° to improve contact between the granules and the heated walls. Microwave and infrared generators can be added to augment the heat transfer rates (34, 35).

Microwave (Dielectric) Drying

By applying microwave energy to pharmaceutical systems to be dried, dielectric materials such as water and solvents with dissolved salts absorb the energy thereby increasing molecular vibration. This movement is in turn converted to friction resulting from interactions with neighboring molecules, solvent temperature increases and ultimately vaporizes, and drying is affected (36). In contrast to previously discussed more conventional means of drying, energy is transferred to the entire volume of solvent in a particle rather than relying on heat transfer from contact surfaces to the interior of a particle or bed. This mode of energy transfer provides for higher temperatures at the center of the granule or powder bed, generating a temperature gradient directed outward from the center of the material. This facilitates both liquid and vapor mass transfer away from the center of the granule. Vaporization of the solvent inside the granule can occur (36), which allows drying rates to be governed by the diffusion coefficient of the solvent vapor rather than that of the liquid, potentially reducing mass transfer limitations in drying rate.

Microwave dryers can be constructed as stand-alone cabinets, as combination dryers with vacuum, fluid bed, or vibrational capabilities, and as one-pot processors that provide mixing and granulation capabilities in conjunction with microwave drying. Microwaves are generated at typical frequencies of either 915 MHz or 2.45 GHz, and are directed to the powder bed to be dried by way of waveguides. The magnetrons used to generate the microwave output require high-voltage supply and may require water cooling to remove excess heat. The size (output) and number of magnetrons depends on the size of the dryer and mass of wet material to be dried, and in many applications are pulsed on and off by a controller to prevent damage to the product resulting from excessive heat generation.

Some dryers also provide heat energy to the powder mass by a jacketed vessel, thereby increasing overall heat transfer. Moisture can be removed via vacuum or hot air fluidization depending on the design of the dryer allowing for improved evaporative drying and vapor mass transfer. Fig. 13 shows the relationship between power input (W) and first-order drying rate constant in a microwave fluid-bed processor (37).

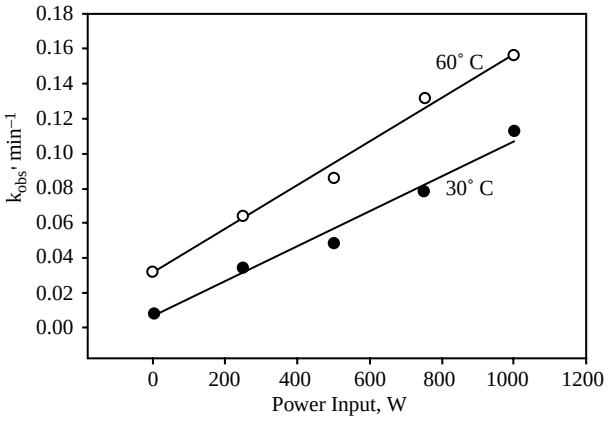

Fig. 13 The influence of microwave power input and inlet air temperature on microwave fluid-bed drying. (From Ref. 37.)

The extent of microwave drying can be correlated to the amount of power absorbed by the product, which is described by Eq. 44 (38):

$$P = 2\pi f V^2 E_0 E_r \tan\delta \tag{44}$$

where P is the power density (W/m^3), f is the frequency (Hz), V the voltage gradient (V/m), E_0 the dielectric constant of vacuum (8.85×10^{-12} F/m), E_r the dielectric constant of the material being dried (F/m), and δ is the loss angle (a physical property of magnetic waves).

The product of the dielectric constant and the loss tangent (tan δ) is called the *loss factor* (36), E_r'', and is a relative measure of how easily a material will be heated by microwave energy.

$$E_r'' = E_r \tan\delta \tag{45}$$

A table of loss factors of some common solvents and excipients are given in Table 3.

Clearly the composition of the powder to be dried plays an integral role in the drying process, using microwaves based on the energy absorption characteristics a formulation possesses. As microwaves penetrate the powder bed the intensity of the electrical field strength is reduced by absorption according to when

$$d = \frac{\lambda_r E_r^{1/2}}{2\pi E_r''} \quad \text{when} \quad E_r'' \ll 1 \tag{46a}$$

or when

$$d = \frac{\lambda_r}{2\pi (E_r'')^{1/2}} \quad \text{when} \quad E_r'' \gg 1 \tag{46b}$$

where d is the depth where the field strength is 37% (or $1/e$) of original value, and λ_r is the wavelength (e.g., 12.3 cm at a frequency of 2450 MHz). Fig. 14 shows the calculated penetration depth for lactose and starch.

Table 3 Comparison of loss factors of some common pharmaceutical materials

Material	Loss factor, E_r''
Methanol	13.6
Ethanol	8.6
Water	6.1
Isopropanol	2.9
Acetone	1.25
Corn starch	0.41
Dibasic calcium phosphate	0.06[a]
Lactose (dry)	0.02, 0.077[b]
Lactose (15% moisture)	0.50[b]

[a]From Ref.(34)
[b]From Ref.(39)
(From Ref. 38 except where indicated.)

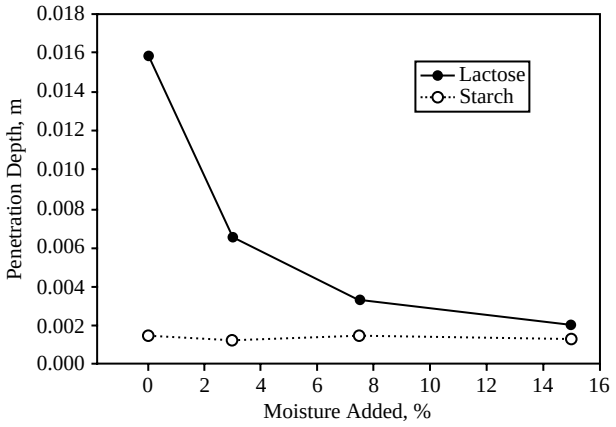

Fig. 14 The effect of moisture on microwave penetration depth. (From Ref. 39.)

Because the penetration depth is limited, both the speed and the uniformity of drying can be improved by mixing during the drying process. As a material loses moisture during the drying process, both its dielectric constant and its loss tangent change. Because the loss factor is the product of these numbers, an understanding of these property characteristics throughout the drying process may be important. For example, starch with 3% moisture has a higher loss factor than it does with both 7.5% and 15% moisture (39).

Theoretical comparisons have been made between conventional drying techniques and microwave and have shown the superior drying rate of microwave over conductive drying in a jacketed bowl (39) and microwave-aided fluid bed-drying over fluid bed-drying alone (40). Because of the reduced drying time associated with the use of increased microwave energy, the generation of pharmaceutical dust can be reduced in a single-pot drying process (41).

Because of the benefits in drying uniformity and efficiency in energy transfer, microwave drying provides an attractive alternative to more conventional modes of drying. For highly potent pharmaceutical compounds the microwave unit provides a high degree of containment (particularly when coupled with high shear granulation) and is an easily cleanable dryer. However, the initial capital investment to install such a dryer and the significant amount of ancillary equipment is oftentimes prohibitive in conventional applications. Nonetheless, uniformity in drying and reduction in time and manpower may be sufficient to consider microwave drying as a viable alternative.

REFERENCES

1. Rohsenow, W.M.; Choi, H.Y. *Heat, Mass, and Momentum Transfer*, Prentice-Hall: Englewood Cliffs, NJ, 1961; 94–98.
2. Carslaw, H.S.; Jaeger, J.C. *Conduction of Heat in Solids*, Oxford University Press: London, 1959.
3. Langhaar, H.L. *Dimensional Analysis and Theory of Models*, John Wiley & Sons: New York, 1951.
4. Kreith, F. *Principles of Heat Transfer*, 3rd Ed.; Intext: New York, 1973; 327–372.
5. Whitaker, S. Forced Convection Heat Transfer Correlations for Flow in Pipes, Past Flat Plates, Single Cylinders, Single Spheres, and for Flow in Packed Beds and Tube Bundles. AIChE J. **1972**, *18*; 361–371.
6. Johnston, H.F.; Pigford, R.L.; Chapin, J.H. Heat Transfer to Clouds of Falling Particles. Univ. Illinois Bull. **1941**, *38* (43); 16–20.
7. Kreith, F. *Principles of Heat Transfer*, 3rd Ed.; Intext: New York, 1973; 445–446.
8. Siegel, R.; Howell, J.R. *Thermal Radiation Heat Transfer*, McGraw-Hill: New York, 1972.
9. Crank, J. *Mathematics of Diffusion*, 2nd Ed.; Oxford University Press: Oxford, 1975; 47–48.
10. Crank, J. *Mathematics of Diffusion*, 2nd Ed.; Oxford University Press: Oxford, 1975; 91.
11. Carstensen, J.T.; Zoglio, M.A. Tray Drying of Pharmaceutical Wet Granulations. J. Pharm. Sci. **1982**, *7* (1), 35–39.
12. Chen, P.; Pei, D.C.T. A Mathematical Model of Drying Process. Int. J. Heat Mass Transfer **1989**, *32* (2), 297–310.
13. Moyers, C.G.; Baldwin, G.W. Psychrometry, Evaporative Cooling, and Solids Drying. *Perry'–s Chemical Engineering Handbook*, 7th Ed.; McGraw-Hill: New York, 1997; 31–33, Ch. 12.
14. Kreith, F. *Principles of Heat Transfer*, 3rd Ed.; Intext: New York, 1973; 596–600.
15. Zografi, G. States of Water Associated with Solids. Drug Dev. Ind. Pharm. **1988**, *14* (14), 1905–1926.
16. Weast, R.C., Ed. *Handbook of Chemistry and Physics*, 70th Ed.; CRC Press: Boca Raton, FL, 1990; D191-D192–D199-D200.
17. Weast, R.C., Ed. *Handbook of Chemistry and Physics*, 70th Ed.; CRC Press: Boca Raton, FL, 1990; C672–C673.
18. Shewmon, P. *Diffusion in Solids*, 2nd Ed.; The Minerals, Metals & Materials Society: Warrendale PA, 1989; 191–215.
19. Kontny, M.J.; Zografi, G. Sorption of Water by Solids. *Physical Characterization of Pharmaceutical Solids*; Brittain, H.G. Ed.; Marcel Dekker, Inc.: New York, 1995; 391–394.
20. Callahan, J.C.; Cleary, G.W.; Elefant, M.; Kaplan, G.; Kensler, T.; Nash, R.A. Equilibrium Moisture Content of Pharmaceutical Excipients. Drug Dev. Ind. Pharm. **1982**, *8* (3), 355–369.
21. Bauer, J.; Quick, J.; Oheim, R.J. Alternate Interpretation of the Role of Water in the Erythromycin Structure. Pharm. Sci. **1985**, *74*, 899.
22. Schilling, R.J. *Abbott Laboratories*, : North Chicago, IL, unpublished.
23. Van Wylen, G.J.; Sonntag, R.E. *Fundamentals of Classical Thermodynamics*, 2nd Ed.; John Wiley & Sons: New York, 1973; 393.
24. *Guidance for Industry, SUPAC-IR/MR: Immediate Release and Modified Release Solid Oral Dosage Forms, Manufacturing Equipment Addendum* CMC 9, Revision 1 U.S. Department of Health and Human Services, Food and Drug Administration, Center for Drug Evaluation and Research: Washington DC, 1999.
25. Cooper, J.; Swartz, C.J.; Suydam, W., Jr. Drying of Tablet Granulations. J. Pharm. Sci. **1961**, *30* (1), 67–75.
26. Wang, Z.H.; Chen, G. Heat and Mass Transfer in Fixed-bed Drying. Chem. Eng. Sci. **1999**, *54*; 4233–4243.
27. Carstensen, J. *Solid Pharmaceutics: Mechanical Properties and Rate Phenomena*, Academic Press: New York, 1980; 149–150.
28. Batchelor, G.K. *An Introduction to Fluid Dynamics*, Cambridge Univ. Press: London, 1970; 229–235.
29. Prandtl, L. *Essentials of Fluid Dynamics*, Blackie & Son: London, 1967; 105–106.
30. White, F. *Viscous Fluid Flow*, McGraw-Hill: New York, 1974; 204–209.
31. Hlinak, A.J.; Saleki-Gerhardt, A. An Evaluation of Fluid Bed Drying of Aqueous Granulations. Pharm. Dev. Tech. **2000**, *5* (1), 11–17.
32. Morris, K.R.; Stowell, J.G.; Byrn, S.R.; Placette, A.W.; Davis, T.D.; Peck, G.E. Accelerated Fluid Bed Drying Using NIR Monitoring and Phenomenological Modeling. Drug Dev. Ind. Pharm. **2000**, *26* (9), 985–988.
33. Moyers, C.G.; Baldwin, G.W. Psychrometry, Evaporative Cooling, and Solids Drying. *Perry'–s Chemical Engineering Handbook*, 7th Ed.; McGraw-Hill: New York, 1997; 65–66, Ch. 12.
34. Duschler, G.; Carius, W.; Bauer, K.H. Single-Step Granulation Method with Microwaves: Preliminary Studies and Pilot Scale Results. Drug Dev. Ind. Pharm. **1995**, *21* (14), 1599–1610.
35. Duschler, G.; Carius, W.; Bauer, K.H. Single-Step Granulation: Development of a Vacuum-Based IR Drying Method (Pilot Scale Results). Drug Dev. Ind. Pharm. **1997**, *23* (2), 119–126.
36. Köblitz, T.; Körblein, G.; Ehrhardt, L. Careful Drying of Temperature-Sensitive Pharmaceutical Granulates in a High-Frequency Field. Pharm. Technol **1986, April, 32**.
37. Doelling, M.K.; Nash, R.A. The Development of a Microwave Fluid-Bed Processor. II. Drying Performance and Physical Characteristics of Typical Pharmaceutical Granulations. Pharm. Res. **1992**, *9* (11); 1493–1501.
38. Doyle, C.; Cliff, M.J. Microwave Drying for Highly Active Pharmaceutical Granules. Manuf. Chem. **1987, February**, 23–32.
39. Vromans, H. Microwave Drying of Pharmaceutical Excipients; Comparison with Conventional Conductive Drying. Eur. J. Pharm. Biopharm. **1994**, *40* (5), 333–336.
40. Wang, Z.H.; Chen, G. Theoretical Study of Fluidized-Bed Drying with Microwave Heating. Ind. Eng. Chem. Res. **2000**, *39*; 775–782.
41. Kiekens, F.; Cordoba-Diaz, M.; Remon, J.P. Influence of Chopper and Mixer Speeds and Microwave Power Level During the High-Shear Granulation Process on the Final Granule Characteristics. Drug Dev. Ind. Pharm. **1999**, *25* (12); 1289–1293.